LTCC FOLD-BACK BANDPASS FILTER DESIGNED WITH CAPACITIVELY LOADED STUBS

K.-S. Chin[1, *], J.-L. Hung[1], C.-W. Huang[1], S.-P. Huang[1], Y.-A. Kao[2], and S.-H. Chao[3]

[1]Department of Electronic Engineering, Chang Gung University, Tao-Yuan 333, Taiwan, R.O.C.

[2]Department of Electrical Engineering, Chang Gung University, Tao-Yuan 333, Taiwan, R.O.C.

[3]Department of Computer Science and Multimedia Design, Taiwan Shoufu University, Tainan 721, Taiwan, R.O.C.

Abstract—This study presents a design of a compact stub-type bandpass filter with capacitively loaded stubs and a fold-back structure. This paper employed the fabrication process of low-temperature co-fired ceramic (LTCC) for filter realization of a multi-layer structure. The proposed filter structure required adding end capacitors to stubs to extend their electrical length, while achieving a length reduction of 30%. This study provided design curves to determine the dimensions of the end capacitor for reaching maximum electrical length extension. In addition, a fold-back configuration was applied to halve the filter size. An experimental filter operating at 5.8 GHz was fabricated and measured to validate the design concept, achieving a highly compact size of $14.3 \times 8.2 \times 0.76 \, \text{mm}^3$.

1. INTRODUCTION

In modern communication systems, the miniaturization of circuits is a significant issue of the development tendency of wireless communication components, which drives the research of compact microstrip filters. Recently, increasing studies have become greatly interested in stub-type bandpass filters due to their advantages of easy fabrication, low cost, compactness, wide bandwidth, and controllable

transmission zeros [1–3]. Stub-type microstrip filters can generally be divided into two main categories. One is designed with fully distributed elements, and the other utilizes mixed lumped/distributed components. Half-wavelength open-circuited resonators and quarter-wavelength short-circuited resonators are most often utilized to be filter resonators, with each having their advantages and disadvantages [1–20].

The structures of applying a defected ground plane to stub-type three-pole bandpass filters [4] or using quarter-wavelength shorted stubs inserting the bandstop filters to substitute for redundant connecting lines [5] were proposed and demonstrated to provide widened bandwidth and stopband. One research by [6] presented an ultra wideband (UWB) filter based on quarter-wave length short-circuited stubs requiring a minimal number of vias, achieving an extremely wide bandwidth of 109%. Zhang et al. [7] developed a wideband bandpass filter with good selectivity using a multimode resonator composed of an open-ended microstrip line with a length of half-wavelength and several radial-line stubs. In reference [8], the study presented an UWB filter with a hybrid microstrip and an implemented slotline structure using a composite series and shunt stubs, possessing higher order transmission poles. The parallel-connected different-length open stubs [9, 10], and stepped-impedance stubs [11, 12], served as the composite shunt resonators to fulfill the dual-band performance. A half-wavelength line with a pair of tap-connected open-ended stubs can be used to build a three-pole bandpass filter with two transmission zeros [13]. Another study [14] presented a UWB filter using five short-circuited stubs with cross-coupling between input and output feed lines. In [15], $\lambda/4$ and short stub-loaded resonators were employed to obtain tri-band responses with independently controlled center frequencies and bandwidths. Most of the aforementioned filters are single-layer with a large circuit size. Accordingly, compact stub-type filters with 3D integrable capability are still preferable for future applications of wireless technologies.

Low-temperature co-fired ceramic (LTCC) technology has recently undergone rapid development due to advantages of 3D schemes, high integrity, fabrication accuracy, and a small size. This study presents a 5.8 GHz $\lambda_g/2$-stub bandpass filter constructed with capacitively loaded stubs and fold-back structures on an LTCC substrate. The proposed capacitive loading can extend the electrical length of stubs effectively, while reducing the physical length by up to 30%. A novel vertical interconnection was developed to vertically fold the filter in half for further size reduction. Also, a prototype was constructed and tested to demonstrate the simplicity of the design.
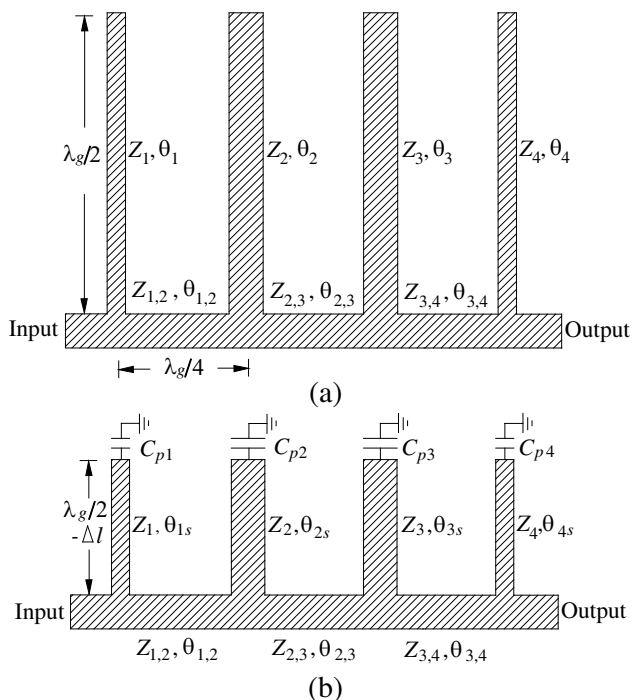
Figure 1. (a) Conventional stub-type fourth-order bandpass filter designed with $\lambda_g/2$ open-circuited stubs connected by $\lambda_g/4$ inverters. (b) The proposed miniaturized bandpass filter constructed with capacitively loaded stubs.

2. DESIGN OF CAPACITIVELY LOADED STUBS

Stub-type microstrip bandpass filters are known for their wide bandwidth, ease of fabrication and good frequency selectivity. This study presents a design of bandpass filters using capacitively loaded stubs for compactness. Figure 1(a) shows the configuration of the conventional fourth-order bandpass filter constructed with $\lambda_g/2$ open-circuited stubs connected by $\lambda_g/4$ inverters. Using $\lambda_g/2$ stubs are advantageous to create transmission zeros at $f_0/2$ and $3f_0/2$, improving frequency selectivity significantly. However, the main disadvantage is its relatively large size in comparison with other types of filters. In our studies, the capacitively loaded stubs and the vertically fold-back structure can be used for size reduction. The stub length was notably reduced from 10 mm to 7 mm achieving a length reduction of 30% by using capacitive loading, while the fold-back structure was further

applied to halve the filter size (from 28.6 mm to 14.3 mm) achieved by vertically folding the filter from its center, which will be explained later.

For compactness, the $\lambda_g/2$ stubs can be replaced with capacitively loaded stubs [19–22] as shown in Figure 1(b). The purpose of adding the capacitor C_p at the stub ends is to lengthen their electrical length, enabling the use of shorter stubs to achieve the same resonance frequency, obtaining a length reduction of up to 30%. Figure 2 shows the configuration of the proposed capacitively loaded stubs on the LTCC substrate, in which only part of the filter is displayed. To save costs and for ease of fabrication, an approximate parallel-plate capacitor structure was adopted. Part of the microstrip stub served as one of the required plates, and another plate with the length of l_p and same width as the stubs was placed above the stub ends separated by a ceramic layer to realize C_p. Enhanced end capacitance results in an extended electrical length Δl, thus reducing the physical length of the stubs significantly. This design provides fully distributed structures throughout, and do not require working separately regarding external lumped capacitors. The radiation loss caused by the open end is also improved since the proposed structure has less of a discontinuity effect.

The extended electrical length Δl can be derived based on the equivalence of input reactance of both transmission lines shown in Figure 3, yielding

$$\Delta l \approx C_p Z_s c / \sqrt{\varepsilon_{reff}} \tag{1}$$

$$\varepsilon_{reff} = \frac{\varepsilon_r + 1}{2} + \frac{\varepsilon_r - 1}{2} \frac{1}{\sqrt{1 + 12\frac{h}{W}}} \tag{2}$$

$$Z_s = \frac{377}{\sqrt{\varepsilon_{reff}}} \left[\frac{W}{h} + 1.393 + 0.677 \ln \left(\frac{W}{h} + 1.444 \right) \right]^{-1} \tag{3}$$
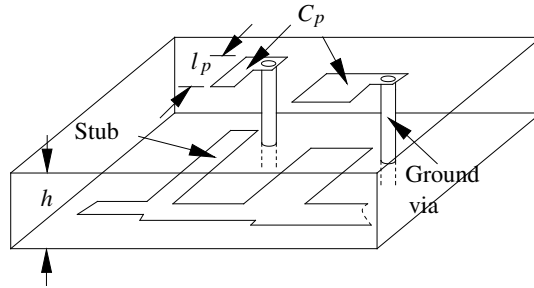

Figure 2. Configuration of the proposed capacitively loaded stubs (only part of the filter is shown).
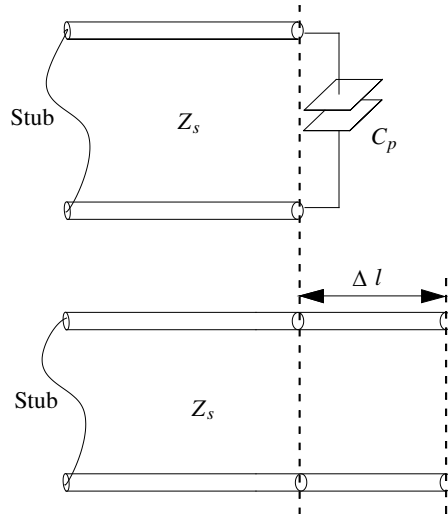
Figure 3. Capacitively loaded stubs and the equivalent length-extended stub.

$$C_p = \frac{\varepsilon_r \varepsilon_0 (W \times l_p)}{h} \tag{4}$$

[1, 2], where c is the speed of light, ε_{reff} denotes the effective dielectric constant, and Z_s is the characteristic impedance of the lines. Equations (1) to (3) reveal that Δl is a function of C_p, Z_s (or the stub width W), the relative dielectric constant ε_r, and the thickness of the substrate h. Since ε_r is fixed by the LTCC fabrication process and Z_s of stubs should be determined by filter specifications, the thinner h can have a larger C_p to attain longer Δl. This work chooses $h = 0.16\,\mathrm{mm}$ for the design of C_p.

By specifying the filter with the fourth-order, $FBW = 20\%$ Chebyshev response, and ripple level of $0.0432\,\mathrm{dB}$, then the design parameters of this filter can be calculated from the synthesis Equations (5)–(12) [1] with the element values of the corresponding low-pass filter prototype, which are as follows: $g_1 = 0.9314$, $g_2 = 1.292$, $g_3 = 1.5775$, $g_4 = 0.7628$, and $g_5 = 1.221$.

$$v_1 = Y_0 g_0 \left(\sqrt{\frac{2g_1}{g_2} + (g_1 \tan \theta)^2} - \sqrt{\frac{2g_1}{g_2}} \right) \tag{5}$$

$$v_n = Y_0 (g_n g_{n+1} - g_0 g_1) \tan \theta$$
$$+ Y_0 g_0 \left(\sqrt{\frac{2g_1 g_{n+1}}{g_0 g_{n-1}} + (g_1 \tan \theta)^2} - \sqrt{\frac{2g_1 g_{n+1}}{g_0 g_{n-1}}} \right) \tag{6}$$

$$v_i = Y_0 g_0 \left(\sqrt{\frac{4g_1^2}{g_{i-1}g_i} + (g_1 \tan \theta)^2} + \sqrt{\frac{4g_1^2}{g_i g_{i+1}} + (g_1 \tan \theta)^2} \right.$$

$$\left. -2g_1 \left(\frac{1}{\sqrt{g_{i-1}g_i}} + \frac{1}{\sqrt{g_i g_{i+1}}} \right) \right), \quad i = 2, \ldots, n-1 \qquad (7)$$

$$Z_i = \left(\frac{v_i(\tan^2 \theta - 1)}{2 \tan^2 \theta} \right)^{-1}, \quad \text{for} \quad i = 1, \ldots, n \qquad (8)$$

$$Z_{1,2} = \left(Y_0 g_0 \sqrt{\frac{2g_1}{g_2}} \right)^{-1} \qquad (9)$$

$$Z_{i,i+1} = \left(Y_0 \frac{2g_0 g_1}{\sqrt{g_i g_{i+1}}} \right)^{-1}, \quad i = 2, \ldots, n-2 \qquad (10)$$

$$Z_{n-1,n} = \left(Y_0 g_0 \sqrt{\frac{2g_1 g_{n+1}}{g_0 g_{n-1}}} \right)^{-1} \qquad (11)$$

$$\theta = \frac{\pi}{2} \left(1 - \frac{FBW}{2} \right) \qquad (12)$$

where n is the filter order and Y_0 is the characteristic admittance. The circuit characteristic parameters are $Z_1 = Z_4 = 21.367\,\Omega$, $Z_2 = Z_3 = 10.769\,\Omega$, $Z_{1,2} = Z_{3,4} = 41.67\,\Omega$, $Z_{2,3} = 38.46\,\Omega$, $\theta_1 = \theta_2 = \theta_3 = \theta_4 = 180°$, and $\theta_{1,2} = \theta_{2,3} = \theta_{3,4} = 90°$. The stub impedances of Z_1, Z_2, Z_3, and Z_4 are mostly of concern for the design of the capacitor C_p. Substituting the stub impedances of $21.367\,\Omega$ and $10.769\,\Omega$, $\varepsilon_r = 7.5$, and $h = 0.16\,\text{mm}$ into (1) (3), yielding C_p as

$$C_{p1}\,(\text{pF}) = C_{p4}\,(\text{pF}) = 0.3805 \times \Delta l\,(\text{mm}) \qquad (13)$$

for the stub impedance of $21.367\,\Omega$, and

$$C_{p2}\,(\text{pF}) = C_{p3}\,(\text{pF}) = 0.7876 \times \Delta l\,(\text{mm}) \qquad (14)$$

for the stub impedance of $10.769\,\Omega$. Figure 4 shows the design curves of C_p versus Δl, ranging from 0–3.5 pF. Extended electrical length Δl increases linearly as C_p increases, with the slope varied with changes in the impedance. For a given C_p, the stub with higher characteristic impedance has more extended electrical length. However, the higher stub impedance is also associated with a narrower line width, resulting in a smaller plate area to reduce C_p, which can be improved by using a longer l_p in the design. A desired Δl can be chosen to find the corresponding value of C_p from Figure 4, so as to implement C_p by using parallel-plate structures. The achievable range of C_p is notably limited by the finite length of microstrip stubs which also serves as a part of the capacitor.
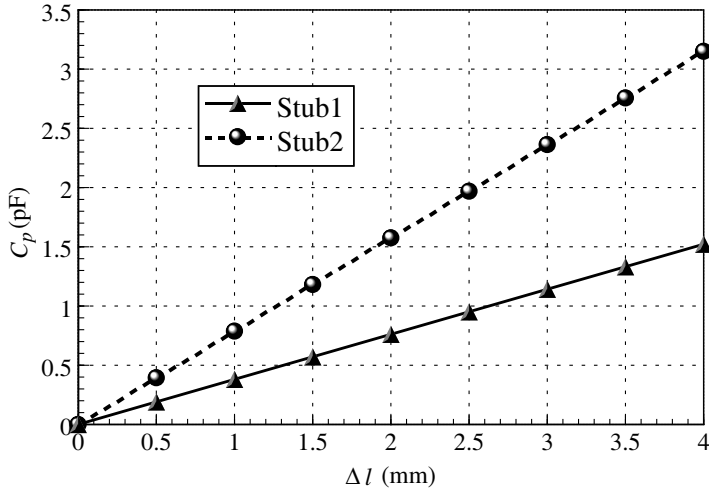
Figure 4. Design curves of C_p versus Δl (Stub 1 with $Z_1 = Z_4 = 21.367\,\Omega$ and Stub 2 with $Z_2 = Z_3 = 10.76\,\Omega$).
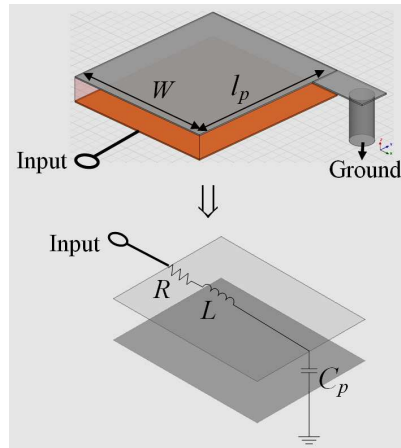

Figure 5. Extraction of capacitance parameters of C_p using an equivalent RLC circuit model fitted with the S_{11}-response of the parallel-plate capacitor.

A rough calculation of circuit dimensions of C_p was conducted from (4). More accurate design curves of l_p versus the capacitance was established for the capacitor design. Since the end capacitor must have the same width as microstrip stubs, only the length of
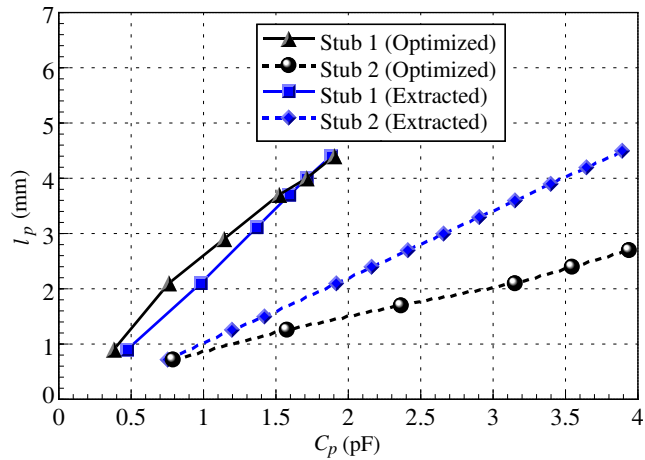
Figure 6. The capacitor length l_p versus C_p, in which Stub 1 with $21.367\,\Omega$ ($W_1 = 0.721\,\text{mm}$) and Stub 2 with $10.769\,\Omega$ ($W_2 = 1.691\,\text{mm}$).
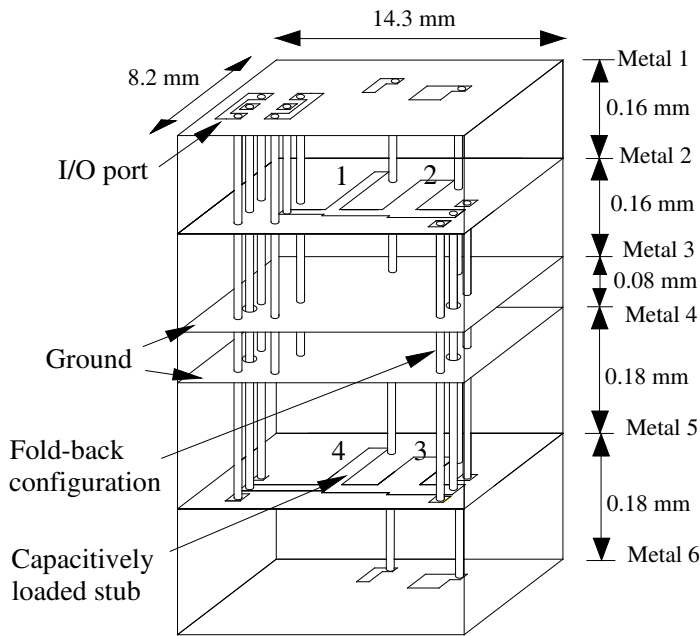

Figure 7. 3D configuration of the proposed LTCC bandpass filter constructed with capacitively loaded stubs and a fold-back structure.
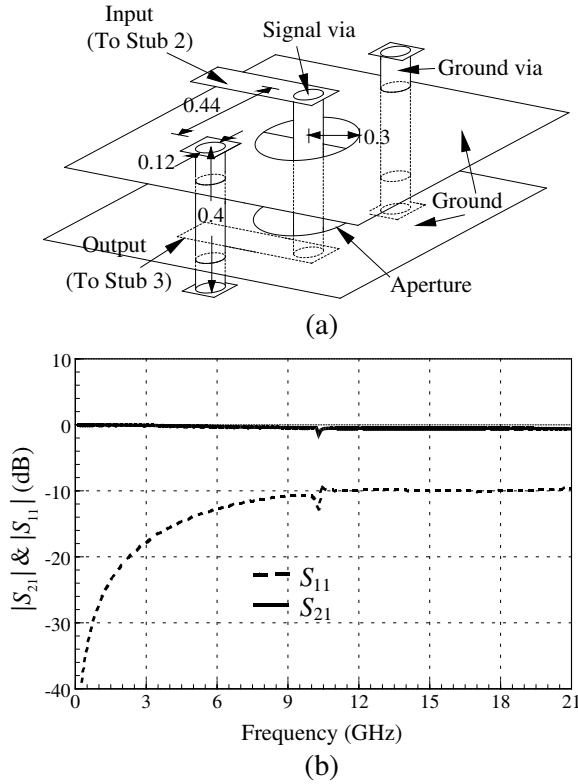
(a)

(b)

Figure 8. (a) 3D configuration of the fold-back structure. (b) Simulated S-parameter responses of the circuit in Figure 8(a).

the plate l_p, required a decision. Figure 5 shows the extraction of capacitance parameters of C_p versus l_p with fixed W, using an equivalent series RLC circuit model fitted with the S_{11}-response of parallel-plate capacitors. The full wave software package HFSS was used for the circuit simulation. Figure 6 displays the extraction results of C_p versus l_p, and are subsequently optimized including the effect of stubs. Stub 2 has a larger difference between the extracted and optimized results due to its wider line width. A desired extended length of Δl can be chosen, and then decide the associated dimension of l_p from Figures 4 and 6. An uplimit of $l_p = 4.4$ mm is present for Stub 1. Since θ_{1s} decreases as l_p increases, an overlong l_p results in insufficient θ_{1s} for the realization of capacitors deteriorating the characteristic of stubs. In this case, l_p is limited to 4.4 mm for obtaining the maximum capacitance without distorting the filter response. The uplimit of l_p

for Stub 2 is 2.7 mm. A length reduction of up to 30% can be achieved by using the proposed capacitively loaded stubs.

3. FOLD-BACK STRUCTURE

The planar filter in Figure 1(b) can be embedded and folded with a multilayer LTCC technology to reduce the size significantly. Figure 7 displays the 3D configuration of the proposed filter constructed with capacitively loaded stubs and a fold-back structure. The filter is vertically folded at its center between Stub 2 and Stub 3 to halve the size. G-S-G pads at I/O ports were designed for RF probing measurements.

A superior fold-back structure was necessary for the connection of stubs. Generally, vias are highly utilized in vertical interconnection structures of high-density system-on-package substrates [23–26]. Field discontinuity may deteriorate the frequency response of filters when signals travel through vias, since the induced parasitic inductance behaves akin to a low-pass filter, attenuating high-frequency components. Smoothing transition structures for field continuity is desired. Adding encircled ground vias around the signal via to form a coaxial-like structure is possible for enhanced field transformation. Reducing dielectric thickness and introducing additional capacitances are also possible solutions to compensate for the parasitic inductance effect. Figure 8(a) shows the proposed three-via fold-back structure: Stub 2 connects to Stub 3 by using a signal via with two ground vias placed at both sides to construct a vertical ground-signal-ground structure. Two apertures on separated grounds with a radius of 0.16 mm were etched allowing the signal via to pass through them. The distance between ground and signal vias is 0.26 mm. Details of the dimensions are labeled in Figure 8(a). Figure 8(b) shows the simulated S-parameter responses achieving an excellent performance of $|S_{11}| > 10$ dB and $|S_{21}| < 0.6$ dB of up to 20 GHz.

4. EXPERIMENTAL FILTER AND MEASUREMENT

For demonstrative purpose, an LTCC 5.8 GHz bandpass filter was confirmed experimentally with specifications of $N = 4$, Chebyshev response, ripple level of 0.0432 dB, and $FBW = 20\%$. This study used the LTCC material provided by the Advanced Ceramic X Corporation, with a relative permittivity of 7.5 and a loss tangent of 0.005, in which the printed conductors were silver. The circuit dimensions including the capacitively loaded stubs were calculated by using the method mentioned in Section 2. The proposed fold-back structure was

applied to reduce the filter size. Figure 7 shows the 3D schematic of the experimental bandpass filter constructed with capacitively loaded stubs and a fold-back structure. This study used six metal layers in the design, separated by five ceramic layers with thicknesses of 0.16 mm, 0.16 mm, 0.08 mm, 0.18 mm, and 0.18 mm, from the top to bottom. The lengths of θ_{1s} and θ_{4s} were notably reduced from 10.3 mm (without the capacitor) to 7.3 mm (with the capacitor, $l_p = 3.1$ mm), and θ_{2s} and θ_{3s} were reduced from 10 mm (without the capacitor) to 7 mm (with the capacitor, $l_p = 1.5$ mm), respectively, achieving a length reduction of 30%. Table 1 lists the physical dimension details. The RF signal was fed and received by G-S-G pads, enabling easy on-chip measurement in which the ground pads were connected further for common ground. The EM full wave software HFSS was used for the simulation.

Figure 9(a) displays the simulated and measured responses of S parameters of the experimental 5.8 GHz bandpass filter, and both results are in close agreement. The measured results show that a slight frequency shift of the central frequency to 5.75 GHz with an insertion loss of 2 dB and return loss of 17 dB. The measured bandwidth was 18% (5.23–6.27 GHz), satisfying the filter specifications. The fourth-order Chebyshev response may notably result in load impedance 61 Ω ($g_5 = 1.221$) causing an impedance mismatch. Fortunately, the situation in this case is not serious, and excellent filter performance is still observed without adding the impedance transformer. Figure 9(b) shows the photographs of Metal 1 and Metal 2 of the experimental filter. The total circuit size, including the input and output G-S-G pads, is $14.3 \times 8.2 \times 0.76$ mm^3.

Table 1. Physical dimensions (in mm) of the experimental filter.

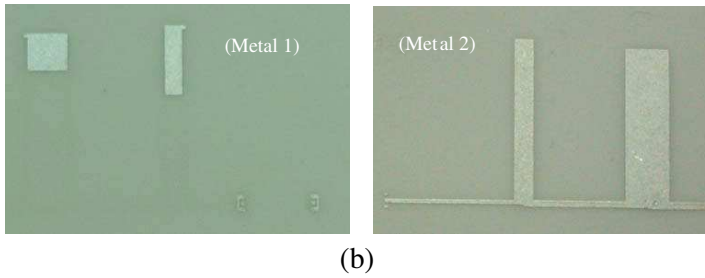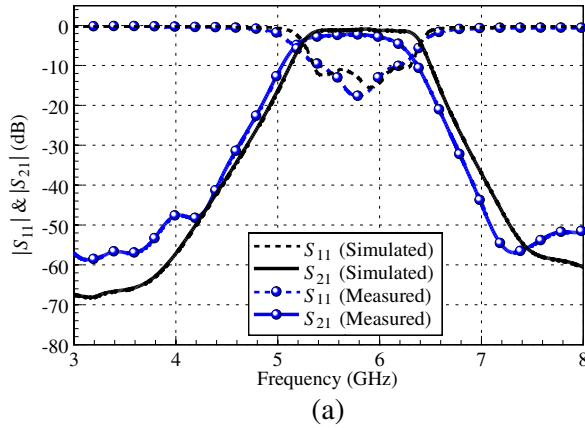| Stub 1 (Z_1, θ_1)		Stub 2 (Z_2, θ_2)		Stub 3 (Z_3, θ_3)		Stub 4 (Z_4, θ_4)	
Length	Width	Length	Width	Length	Width	Length	Width
7.3	0.721	7.0	1.691	7.0	1.903	7.3	0.811
Connecting Line ($Z_{1,2}, \theta_{1,2}$)		Connecting Line ($Z_{2,3}, \theta_{2,3}$)		Connecting Line ($Z_{3,4}, \theta_{3,4}$)		C_{p1}	
Length	Width	Length	Width	Length	Width	Length	Width
5.406	0.26	5.38	0.3	5.406	0.293	2.9	0.721
C_{p2}		C_{p3}		C_{p4}		Via Diameter	Via Spacing
Length	Width	Length	Width	Length	Width	Diameter	Spacing
1.7	1.691	2.9	1.903	1.7	0.811	0.12	0.26

(a)

(b)

Figure 9. (a) Simulated and measured responses of S parameters of the experimental LTCC 5.8 GHz bandpass filter. (b) Photographs of Metal 1 and 2 of the experimental filter.

5. CONCLUSIONS

This study presents a design of a 5.8 GHz LTCC bandpass filter with capacitively loaded stubs for compactness. The filters added capacitances at the end of the stubs to extend their electrical length, achieving a length reduction of up to 30%. Design curves were provided to determine the circuit dimensions of end capacitors for appropriate electrical length extension. This paper also developed a novel vertical interconnection to further reduce the filter size by 50%, achieved by vertically folding the filter from its center. The design concept was demonstrated by fabricating an experimental fourth-order LTCC bandpass filter that yielded a low insertion loss of 2 dB, a bandwidth of 18%, and a return loss of 17 dB.

ACKNOWLEDGMENT

REFERENCES

1. Hong, J.-S. and M. J. Lancaster, *Microstrip Filters for RF/Microwave Application Engineering*, John Wiley & Sons, New York, 2001.

2. Chang, K., I. Bahl, and V. Nair, *RF and Microwave Circuit and Component Design for Wireless Systems*, John Wiley & Sons, New York, 2002.

3. Matthaei, G. L., L. Young, and E. M. T. Johns, *Microwave Filters, Impedance Matching Networks, and Coupling Structures*, Artech House, Norwood, MA, 1980.

4. Abdel-Rahman, A., A. K. Verma, A. Boutejdar, and A. S. Omar, "Compact stub type microstrip bandpass filter using defected ground plane," *IEEE Microwave and Wireless Components Letters*, Vol. 14, No. 4, 136–138, 2004.

5. Lin, W.-J., C.-S. Chang, J.-Y. Li, D.-B. Lin, L.-S. Chen, and M.-P. Houng, "Improved compact broadband bandpass filter using branch stubs co-via structure with wide stopband characteristic," *Progress In Electromagnetics Research C*, Vol. 5, 45–55, 2008.

6. Razalli, M. S., A. Ismail, M. A. Mahdi, and M. N. Bin Hamidon, "Novel compact microstrip ultra-wideband filter utilizing short-circuited stubs with less vias," *Progress In Electromagnetics Research*, Vol. 88, 91–104, 2008.

7. Zhang, L., Z.-Y. Yu, and S.-G. Mo, "Novel planar multimode bandpass filters with radial-line stubs," *Progress In Electromagnetics Research*, Vol. 101, 33–42, 2010.

8. Li, R., S. Sun, and L. Zhu, "Synthesis design of ultra-wideband bandpass filters with composite series and shunt stubs," *IEEE Trans. Microwave Theory Tech.*, Vol. 51, 684–692, 2009.

9. Ma, Z., K. Kikuchi, Y. Kobayashi, T. Anada, and G. Hagiwara, "Novel microstrip dual-band bandstop filter with controllable dual-stopband response," *Proceedings of Asia-Pacific Microwave Conference*, 1177–1180, 2006.

10. Tsai, C.-M., H.-M. Lee, and C.-C. Tsai, "Planar filter design with fully controllable second passband," *IEEE Trans. Microwave Theory Tech.*, Vol. 53, 3429–3439, 2005.

11. Chin, K.-S. and C.-K. Lung, "Miniaturized microstrip dual-band bandstop filters using tri-section stepped-impedance resonators," *Progress In Electromagnetics Research C*, Vol. 10, 37–48, 2009.

12. Chin, K.-S. and J.-H. Yeh, "Dual-wideband bandpass filter using short-circuited stepped-impedance resonators," *IEEE Microwave and Wireless Components Letters*, Vol. 19, No. 3, 155–157, 2009.

13. Quendo, C., E. Rius, and C. Person, "Narrow bandpass filters using dual-behavior resonators," *IEEE Trans. Microwave Theory Tech.*, Vol. 51, 734–743, 2003.

14. Zhu, L. and W. Menzel, "Compact microstrip bandpass filter with two transmission zeros using a stub-tapped half-wavelength line resonator," *IEEE Microwave and Wireless Components Letters*, Vol. 13, 1618, 2003.

15. Lin, X.-M., "Design of compact tri-band bandpass filter using $\lambda/4$ and stub-loaded resonators," *Journal of Electromagnetic Waves and Applications*, Vol. 24, Nos. 14–15, 2029–2035, 2010.

16. Velázquez-Ahumada, M. D. C., J. Martel-Villagr, F. Medina, and F. Mesa, "Application of stub loaded folded stepped impedance resonators to dual band filters," *Progress In Electromagnetics Research*, Vol. 102, 107–124, 2010.

17. Liu, C.-Y., T. Jiang, and Y.-S. Li, "A novel UWB filter with notch-band characteristic using radial-UIR/SIR loaded stub resonators," *Journal of Electromagnetic Waves and Applications*, Vol. 25, Nos. 2–3, 233–245, 2011.

18. Yin, Q., L.-S. Wu, L. Zhou, and W.-Y. Yin, "Compact dual-band bandpass filter using asymmetrical dual stub-loaded open-loops," *Journal of Electromagnetic Waves and Applications*, Vol. 24, Nos. 17–18, 2397–2406, 2010.

19. Liu, H., R. H. Knoechel, and K. F. Schuenemann, "Miniaturized bandstop filter using meander spurline and capacitively loaded stubs," *ETRI Journal*, Vol. 29, No. 5, 2007.

20. Drozd, J. M. and W. T. Joines, "A capacitively loaded half-wavelength tapped-stub resonator," *IEEE Trans. Microwave Theory Tech.*, Vol. 45, No. 7, 1100–1104, 1997.

21. Hoa, D. T. and I. S. Kim, "Miniaturized low insertion loss multilayer capacitively loaded step-impedance interdigital bandpass filter," *Proceedings of Asia Pacific Microwave Conference*, 1–4, 2007.

22. Görür, A., C. Karpuz, and M. Akpinar, "A reduced-size dual-mode bandpass filter with capacitively loaded open-loop arms," *IEEE Microwave and Wireless Components Letters*, Vol. 13, No. 9, 385–387, 2003.

23. Stark, A. and A. F. Jacob, "A broadband vertical transition for millimeter-wave applications," *Proceedings of the 38th European Microwave Conference*, 476–479, 2008.

24. Valois, R., et al., "High performances of shielded LTCC vertical transitions from DC up to 50 GHz," *IEEE Trans. Microwave Theory Tech.*, Vol. 53, No. 6, 2026–2032, 2005.

25. Yang, T.-H., C.-F. Chen, T.-Y. Huang, C.-L. Wang, and R.-B. Wu, "A 60 GHz LTCC transition between microstrip line and substrate integrated waveguide," *Proceedings of Asia Pacific Microwave Conference*, 3, 2005.

26. Lee, Y. C., "CPW-to-stripline vertical via transitions for 60 GHz LTCC SoP applications," *Progress In Electromagnetics Research Letters*, Vol. 2, 37–44, 2008.